

# From Point to probabilistic gradient boosting for claim frequency and severity prediction

Dominik Chevalier<sup>1</sup> and Marie-Pier Côté<sup>1</sup>

<sup>1</sup>École d'actuariat, Université Laval, 2425, rue de l'Agriculture, Québec, QC, Canada, G1V 0A6.

Corresponding author: Dominik Chevalier (dominik.chevalier.1@ulaval.ca)

December 20, 2024

## Abstract

Gradient boosting for decision tree algorithms are increasingly used in actuarial applications as they show superior predictive performance over traditional generalized linear models. Many improvements and sophistications to the first gradient boosting machine algorithm exist. We present in a unified notation, and contrast, all the existing point and probabilistic gradient boosting for decision tree algorithms: GBM, XGBoost, DART, LightGBM, CatBoost, EGBM, PGBM, XGBoostLSS, cyclic GBM, and NGBoost. In this comprehensive numerical study, we compare their performance on five publicly available datasets for claim frequency and severity, of various size and comprising different number of (high cardinality) categorical variables. We explain how varying exposure-to-risk can be handled with boosting in frequency models. We compare the algorithms on the basis of computational efficiency, predictive performance, and model adequacy. LightGBM and XGBoostLSS win in terms of computational efficiency. The fully interpretable EGBM achieves competitive predictive performance compared to the black box algorithms considered. We find that there is no trade-off between model adequacy and predictive accuracy: both are achievable simultaneously.<sup>2,3</sup>

## 1 Introduction

While generalized linear models (GLMs) have been the cornerstone of general insurance ratemaking for many years [10, 21], recent advancements in machine learning provide actuaries with a wide range of competing predictive algorithms. In particular, gradient boosting machine (GBM) can improve predictive performance over GLMs for risk segmentation [31]. Gradient boosting proliferates in actuarial applications, such as auto insurance [8, 24], hierarchical non-life reserving [9], and health insurance [28, 27].

GBM, proposed by Friedman [22], is a predictive algorithm that combines weak learners, simple models that are usually decision trees, to gradually improve predictions by leveraging gradient descent, an optimisation technique. The enhanced precision of GBM comes with the cost of an opaque computationally intensive algorithm. Many refinements of gradient boosting for decision trees (GBDT) tackle computational efficiency, such as XGBoost [6] and LightGBM [35], the treatment of categorical variables, such as CatBoost [50], and model interpretability, such as explainable GBM (EGBM) [38, 39].

The above GBDT algorithms perform point prediction, which, in most cases, leads to an estimator of the expected response variable conditional on covariates. They do not describe the general behaviour of the response variable and its distribution, crucial elements for risk management purposes in actuarial modelling. As an alternative, in their “recent challenges in actuarial science”, Embrechts and Wüthrich [18] recommend transitioning towards probabilistic prediction for a better uncertainty assessment. In [45], this idea is used for

<sup>2</sup>Keywords: Gradient boosting for decision trees, Interpretability, Model adequacy, Predictive modelling, Proper scoring rules.

<sup>3</sup>JEL classification: C6, G22, G52.

the construction of a dual-parameter tree boosting method to emulate the GLM framework with zero-inflated data, an approach generalized in cyclic GBM (cyc-GBM) [11]. Probabilistic gradient boosting techniques were applied in the context of zero-inflated insurance claim frequency [57, 48], and along with copula models for multivariate claim severities [48].

From the machine learning angle, Breiman [2] opposes the “Data modelling culture”, in which we try to understand the probabilistic distribution of the data, to the “Algorithmic modelling culture”, in which we aim to estimate accurate predictor functions regardless of distributional assumptions. The line between the two cultures is blurry with the rise of probabilistic forecasting models: motivated by reconciling these cultures, März [41] proposes XGBoostLSS, that sequentially runs XGBoost algorithms for multi-parameter predictions. This is the first of many probabilistic GBDT algorithms, whose objective is to predict distributional parameters given covariates. In the same vein, Delong et al. [11] take advantage of the cyclic coordinate descent optimisation algorithm in cyc-GBM. Because the gradient is not invariant to reparametrization, Duan et al. [16] replace it by a rescaled version in their natural gradient boosting (NGBoost) algorithm. Predicting the expectation and variance is the focus in the probabilistic GBM algorithm PGBM [58], built in the XGBoost framework.

In this comprehensive review, we present in a unified notation the point and probabilistic GBDT algorithms, and compare their performance in a numerical study on a variety of insurance datasets. We explain the passage from a point prediction to a predicted distribution per observation. We examine five point prediction GBDT approaches (GBM, XGBoost, LightGBM, CatBoost, and EGBM) and four probabilistic algorithms (XGBoostLSS, cyc-GBM, NGBoost and PGBM). We show how varying exposure-to-risk can be handled in GBDT frequency models. We also perform a numerical study on claim frequency and severity data with five publicly available datasets resulting in a novel impartial comparative analysis of these algorithms on the basis of computational efficiency, predictive performance, and model adequacy. We find that LightGBM stands out as the most computationally efficient with little or no loss in predictive performance. Amongst the probabilistic algorithms, XGBoostLSS is the most computationally efficient while providing adequate fit in terms of the coverage of confidence intervals. Interestingly, the probabilistic GBDT algorithms can enhance model adequacy without hindering predictive performance. Although all algorithms achieve similar predictive performance, CatBoost can lead to a small improvement when the dataset contains many high cardinality categorical variables.

Probabilistic GBDT refinements are developed concurrently and introduced in the literature with different notations, making it difficult for users to grasp their similarities and particularities. Our contribution is two-fold. First, our comprehensive review presents the probabilistic GBDT algorithms in a coherent and consistent manner. Second, our numerical study on claim frequency and severity data is impartial and sheds light on computational efficiency, predictive performance, and model adequacy, the latter being rarely studied in conjunction with GBDT. We use five different datasets and ten GBDT algorithms, some of which have never been compared.

The remainder of this paper is structured as follows. To establish the basis of the two types of GBDT algorithms, we distinguish point and probabilistic predictions in Section 2. Then, we describe the GBDT algorithms in Section 3. The experimental setup and performance metrics are presented in Section 4. Section 5 contains the numerical comparative study, and a discussion follows in Section 6. The tuning procedure is detailed in Appendix A and additional results are available in Appendix B.

## 2 From point to probabilistic prediction

Let  $Y$  be a response variable, i.e., the target, and  $\mathbf{x}$  be the associated  $\eta$ -dimensional vector of covariates. Let  $\mathcal{D} = \{(\mathbf{x}_i, y_i) : i = 1, \dots, n\}$  be a dataset of  $n$  independent copies of  $(\mathbf{x}, Y)$ . GBDT algorithms solve a supervised learning task and rely on a pre-specified loss function. For observation  $i \in \{1, \dots, n\}$ , the loss function  $\mathcal{L}(y_i, b_i)$  takes two arguments: the observed target  $y_i$  and a candidate prediction  $b_i$  that may depend on  $\mathbf{x}_i$ . The GBDT training algorithms iteratively update the candidate predictions  $b_1, \dots, b_n$ , in an attempt to minimize the total loss for  $\mathcal{D}$ , defined as  $\sum_{i=1}^n \mathcal{L}(y_i, b_i)$ . The possibility of choosing any loss function makes gradient boosting versatile.

The squared error loss  $\mathcal{L}(y_i, b_i) = (y_i - b_i)^2$  is commonly used to tackle regression tasks. Optimising the total squared error loss amounts to an ordinary least squares (OLS) procedure or a maximum likelihood

estimation (MLE) of the location parameter of an elliptical distribution (e.g., a Gaussian distribution). However, because symmetric distributions are rarely appropriate for claim severity and frequency modelling, other loss functions like the gamma or Poisson deviances should be considered [65]. For observation  $i$ , the gamma deviance is given by

$$\mathcal{L}(y_i, b_i) \propto \left( \frac{y_i - b_i}{b_i} - \ln \frac{y_i}{b_i} \right),$$

and the Poisson deviance is

$$\mathcal{L}(y_i, b_i) \propto \left\{ y_i \ln \left( \frac{y_i}{b_i} \right) - (y_i - b_i) \right\},$$

where we impose that  $y_i \ln y_i = 0$  if  $y_i = 0$  [see, e.g., 13]. The family for the conditional distribution of  $Y$  is implied by the choice of loss function. Like for the squared error loss, which can be viewed as the Gaussian deviance, the minimum of these deviances is attained at  $b_i = E[Y_i | \mathbf{x}_i]$ . Therefore, the learned prediction function when the objective is the total deviance can be interpreted as an estimator  $\hat{\mu}(\mathbf{x})$  of  $E[Y | \mathbf{x}]$ . It would be possible to specify a loss function to perform quantile regression as seen, e.g., in [20, 61], but we focus on point predictions for the conditional expectation.

In the OLS framework, after the estimation of the regression coefficients, we get point predictions for  $\hat{\mu}(\mathbf{x})$ . Given these  $\hat{\mu}(\mathbf{x}_1), \dots, \hat{\mu}(\mathbf{x}_n)$ , the (constant) variance parameter can be estimated by maximizing the log-likelihood under the assumption of homoscedasticity. Similarly, given predicted means  $\hat{\mu}(\mathbf{x}_1), \dots, \hat{\mu}(\mathbf{x}_n)$  from a GBDT algorithm, other (constant) distributional parameters can be estimated by maximizing the log-likelihood under a homogeneity assumption. This last assumption means that scale and/or shape parameters do not vary with  $\mathbf{x}$ . This way, we obtain a predicted distribution per observation, leveraging point prediction to build probabilistic models.

To relax the homogeneity and linearity assumptions in GLMs, Rigby and Stasinopoulos [52] propose generalized additive models for location, scale, and shape (GAMLSS). They allow all the parameters of the conditional distribution of  $Y$  given  $\mathbf{x}$  to be modelled by smooth functions of the covariates. GAMLSS equips us for “more flexible modelling of more suitable distributions” [60] in the actuarial context, so it is natural to combine the flexibility of GAMLSS with the predictive potential of GBDT. To this end, probabilistic GBDT algorithms can predict all the distributional parameters as functions of  $\mathbf{x}$ , thereby granting them with the advantages of GAMLSS noted above. In addition, most distributions may be parametrised by a mean (often the location) parameter, whose estimate corresponds to a point prediction. Thus, probabilistic GBDT algorithms yield point predictors as a by-product of the estimated distribution.

### 3 Survey of gradient boosting for decision trees

Gradient boosting stems from Schapire’s “strength of weak learnability” [53], a theory in which the iterative summation of simple models, called weak learners, can form strong predictive models. Friedman [22] proposes the classification and regression trees (CART) of Breiman et al. [3] as weak learners in a gradient descent procedure. In such a GBDT algorithm, we aggregate a predetermined number  $M$  of simple decision trees to obtain the flexible GBDT predictor function

$$f_{\text{GBDT}}^M(\mathbf{x}) = f_{\text{GBDT}}^{M-1}(\mathbf{x}) + h_M(\mathbf{x}) = \sum_{m=1}^M h_m(\mathbf{x}),$$

where  $h_m(\mathbf{x})$  is the prediction function of the decision tree in the  $m$ th iteration. Some enhancements follow Friedman’s method [22]: they tackle its lack of transparency, the computational weaknesses of the CART weak learners, and probabilistic prediction. Fig. 1 is a comprehensive concept map of the implementations of GBDT. Note that we only consider gradient boosting, and not other types such as Delta boosting [37].

**Remark 1.** *When the domain of the target parameter, say  $\mu$ , is not  $\mathbb{R}$ , we introduce a link function  $\varphi$  to properly restrict the prediction to the desired set. We express the loss function  $\mathcal{L}(y, b)$  such that  $b = \varphi(\mu) \in \mathbb{R}$  under the chosen link function. The output prediction function of the GBDT is then*

$$\hat{\mu}(\mathbf{x}) = f_{\text{GBDT}}(\mathbf{x}) = \varphi^{-1}\{f_{\text{GBDT}}^M(\mathbf{x})\}.$$

*It is common to use the log link  $\varphi(x) = \log(x)$  for a positive target parameter.*

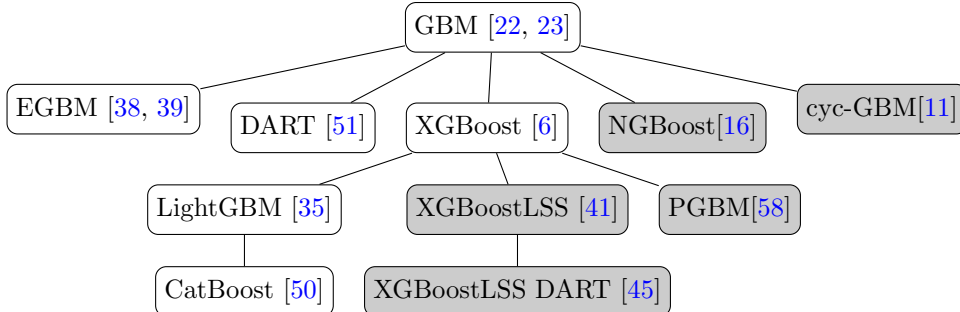


Figure 1: Comprehensive concept map of point (white) and probabilistic (grey) GBDT algorithms.

In this section, we review GBDT algorithms. In Section 3.1, we describe point prediction GBDT algorithms, including computational enhancements and the issue of model interpretability. Probabilistic GBDT methods are presented in Section 3.2: XGBoostLSS, cyc-GBM, and NGBoost. We discuss hybrid strategies in Section 3.3.

### 3.1 Gradient boosting machines and their enhancements for point prediction

Algorithm 1 presents stochastic gradient boosting machine (GBM), the root of the concept map in Fig. 1, introduced in [22, 23]. The way we present the algorithm follows [29]. We use the indicator function  $\mathbf{1}(A) = 1$  if  $A$  is true and 0 otherwise. To train the predictor function for modelling  $Y$ , we specify hyperparameters  $\delta, \lambda, d$ , and  $M$ . The performance of the algorithm varies greatly with tree depth  $d$  and number of boosting iterations  $M$ : tuning them carefully is important. The results are less sensitive to the subsampling percentage  $\delta$  and the learning rate  $\lambda$ , as long as they are fixed to reasonable values. We detail below the role of each hyperparameter.

In Step 1 of Algorithm 1, we initialise  $f^0(\mathbf{x})$  at the constant  $b$  which minimizes the total loss for  $\mathcal{D}$ , the training set comprising  $n$  records. Friedman [23] introduces stochastic gradient boosting machines to prevent overfitting: in each iteration  $m \in \{1, \dots, M\}$ , we fit a decision tree on  $\mathcal{D}'$ , a random subsample of size  $\delta n$  from  $\mathcal{D}$ . For  $i \in \mathcal{D}'$  in the  $m$ th iteration, we evaluate pseudo-residuals, defined as the gradient of the loss function evaluated at the previous iteration’s prediction  $f^{m-1}(\mathbf{x}_i)$ , indicating the direction towards minimal loss:

$$g_i = - \left. \frac{\partial \mathcal{L}(y_i, b)}{\partial b} \right|_{b=f^{m-1}(\mathbf{x}_i)}. \quad (1)$$

In the learning phase, decision trees of depth  $d$  are fitted to the pairs  $\{(\mathbf{x}_i, g_i) : i \in \mathcal{D}'\}$  with the mean squared error criterion — regardless of the loss function  $\mathcal{L}$  — to partition the covariate space into regions with homogenous gradient values  $g_i$ . We emphasize that the target  $g_i$  reflects how “well-trained” the  $i$ th observation is in iteration  $m$ : it changes with  $m$  even though we drop the index for simplicity of notation. Observations in undertrained regions of the covariate space have high absolute gradients, implying a large influence on the optimal tree splits due to the squared error criterion. Then, for terminal region  $j \in \{1, \dots, J_m\}$ , we find the optimal step towards minimal loss, denoted  $\hat{b}_j^m$ . We update the prediction  $f^{m-1}(\mathbf{x})$  for  $\mathbf{x} \in R_j^m$  by adding  $\hat{b}_j^m$ , shrunk by a learning rate  $\lambda \in (0, 1]$ . We use the `gbm3` R implementation [32].

The learning rate, also known as the shrinkage parameter, helps convergence by preventing overly large steps and by avoiding local optima or saddle points. Shrinkage is a form of regularization that mitigates over-specialization, that is, when late iterations contribute effectively to the prediction of very few observations. Yet, Rashimi and Gilad-Bachrach [51] find that shrinkage does not completely overcome this issue. They propose the Dropout meets multiple Additive Regression Trees (DART) algorithm, inspired by the dropout approach used for neural networks [59]. They drop a proportion of the previous boosting iterations to evaluate the gradients, corrected by a scaling factor, instead of using  $f^{m-1}(\mathbf{x}_i)$  in Step 4 of Algorithm 1. DART involves hyperparameters to control the proportion and periodicity of the dropout. Rashimi and Gilad-Bachrach [51] find that DART succeeds in tackling the over-specialization problem in GBDT, sometimes

---

**Algorithm 1:** Stochastic gradient boosting machine for decision trees

---

**Inputs:**  $\mathcal{L}, \varphi, \mathcal{D}, \delta, \lambda, d,$  and  $M$ .

1 Initialise  $f^0(\mathbf{x}) = \operatorname{argmin}_b \sum_{i=1}^n \mathcal{L}(y_i, b)$ .

2 **for**  $m = 1$  **to**  $M$  **do**

3     Sample  $\mathcal{D}'$ , a subset of  $\delta n$  observations without replacement from  $\mathcal{D}$ .

4     Compute  $g_i$  with Eq. (1) for  $i \in \mathcal{D}'$ .

5     Fit tree of depth  $d$  to  $\{(\mathbf{x}_i, g_i) : i \in \mathcal{D}'\}$  to get terminal regions  $R_1^m, \dots, R_{J_m}^m$ .

6     Compute, for  $j \in \{1, \dots, J_m\}$ ,

$$\hat{b}_j^m = \operatorname{argmin}_b \sum_{i \in \mathcal{D}' : \mathbf{x}_i \in R_j^m} \mathcal{L}\{y_i, f^{m-1}(\mathbf{x}_i) + b\}.$$

7     Update  $f^m(\mathbf{x}) = f^{m-1}(\mathbf{x}) + \lambda \sum_{j=1}^{J_m} \hat{b}_j^m \mathbf{1}(\mathbf{x} \in R_j^m)$ .

8 **Return :** Prediction function  $f_{\text{GBM}}(\mathbf{x}) = \varphi^{-1}\{f^M(\mathbf{x})\}$ .

---

improving predictive performance over the use of a shrinkage parameter, at the cost of being computationally intensive.

It is found in [31] that GBMs improve performance over GLMs in insurance applications, most likely due to their flexibility and ability to automatically handle complex ( $d > 1$ ) non-linear effects. Yet, GBMs are computationally intensive: each iteration involves an exhaustive search for CART splits and exact gradient evaluations.

### 3.1.1 Computational enhancements

Motivated by improving the scalability of the GBM algorithm, Chen and Guestrin [6] propose XGBoost. They leverage parallel programming and a simplified split-finding algorithm based on a quantile sketch of the gradients. XGBoost also optimises a second order Taylor approximation of the loss function with two regularisation parameters:  $\gamma$ , the minimal loss function reduction required for a tree split, and  $\phi$ , the  $\ell_2$  penalty on the tree predictions. The XGBoost objective in iteration  $m \in \{1, \dots, M\}$  is

$$\sum_{i \in \mathcal{D}'} \left\{ g_i h_m(\mathbf{x}_i) + t_i \frac{h_m(\mathbf{x}_i)^2}{2} \right\} + \gamma J_m + \frac{1}{2} \phi \sum_{j=1}^{J_m} (b_j^m)^2,$$

where the gradient  $g_i$  is defined in Eq. (1), the Hessian of the loss function is

$$t_i = - \left. \frac{\partial^2 \mathcal{L}(y_i, b)}{\partial b^2} \right|_{b=f^{m-1}(\mathbf{x}_i)}, \quad (2)$$

the decision tree prediction function is

$$h_m(\mathbf{x}_i) = \sum_{j=1}^{J_m} b_j^m \mathbf{1}(\mathbf{x}_i \in R_j^m),$$

and  $b_j^m$  is the weight of leaf  $j \in \{1, \dots, J_m\}$ . The  $j$ th optimal leaf weight is

$$\hat{b}_j^m = \frac{\sum_{i \in \mathcal{D}' : \mathbf{x}_i \in R_j^m} g_i}{\sum_{i \in \mathcal{D}' : \mathbf{x}_i \in R_j^m} t_i + \phi}. \quad (3)$$

Indeed, the Taylor approximation allows to compute these tree predictions in closed form, speeding up the training even though we compute the Hessian on top of the gradient. We write the XGBoost procedure of [6]

with our notation in Algorithm 2. As in random forest [1], column subsampling can be used to reduce the dimensionality of the set of potential splits when building the tree in Step 5 of Algorithm 2. For this study, we use the R implementation in package `xgboost` [7].

---

**Algorithm 2:** XGBoost

---

**Inputs:**  $\mathcal{L}, \varphi, \mathcal{D}, \delta, \zeta, \lambda, d, M, \gamma$ , and  $\phi$ .

- 1 Initialise  $f^0(\mathbf{x}) = \operatorname{argmin}_b \sum_{i=1}^n \mathcal{L}(y_i, b)$ .
  - 2 **for**  $m = 1$  **to**  $M$  **do**
  - 3     Sample  $\mathcal{D}'$ , a subset of  $\delta n$  observations without replacement from  $\mathcal{D}$ .
  - 4     Compute  $g_i$  and  $t_i$  with Eqs (1) and (2) for  $i \in \mathcal{D}'$ .
  - 5     Fit tree of depth  $d$  to  $\{(\mathbf{x}_i, g_i) : i \in \mathcal{D}'\}$  with column subsampling  $\zeta$ , minimal loss reduction  $\gamma$  and the simplified split-finding algorithm of [6] to get terminal regions  $R_1^m, \dots, R_{J_m}^m$ .
  - 6     Compute  $\hat{b}_j^m$  using Eq. (3) for  $j \in \{1, \dots, J_m\}$ .
  - 7     Update  $f^m(\mathbf{x}) = f^{m-1}(\mathbf{x}) + \lambda \sum_{j=1}^{J_m} \hat{b}_j^m \mathbf{1}(\mathbf{x} \in R_j^m)$ .
  - 8 **Return** : Prediction function  $f_{\text{XGBoost}}(\mathbf{x}) = \varphi^{-1}\{f^M(\mathbf{x})\}$ .
- 

LightGBM [35] and CatBoost [50] are enhancements of XGBoost. Both modify the tree growth strategy for Step 5 of Algorithm 2. In LightGBM, Ke et al. [35] aim to enhance computational efficiency in handling categorical features more succinctly, sophisticating the sampling step, and growing trees leafwise. CatBoost [50] is designed for datasets with numerous, possibly imbalanced, categorical variables. It addresses GBDT algorithms’ predictive shift, a bias proportional to  $1/n$ . In [57], it is highlighted that CatBoost is suited for actuarial modelling because of the attention drawn to categorical features. A qualitative and quantitative comparative analysis of XGBoost, LightGBM, and CatBoost can be found in [56]. We experiment with the R implementations `lightgbm` [54] and `catboost` [15].

**Remark 2.** *Second order Taylor approximation of the loss is called Newton boosting. According to Sigrist [55], it can improve predictive performance. Gradient and Newton boosting are used interchangeably in literature, which is criticized in [55]. In Fig. 1, all the algorithms that are descendents of XGBoost use Newton steps.*

### 3.1.2 An interpretable alternative

GBDT algorithms with deep trees as weak learners are complex black boxes. Unlike GLMs, they do not output parameter estimates describing each covariate effect on the prediction. Also, high order interactions make it impossible for the human brain to conceptualize these effects. Thus, actuaries cannot directly explain a tariff structure output from a GBDT loss cost model, as may be required by stakeholders or by regulation [e.g., 25]. They must rely on—possibly misleading [67]—explanation tools.

Transparent models can be obtained by taking a depth of  $d = 1$  in GBDT algorithms, because tree stumps split the covariate space according to only one feature at a time. To this end, Lou et al. [39, 38] build a generalized additive model (GAM) based on feature-wise effects (boosted tree stumps) and pairwise interactions: Generalized Additive Model plus Interactions. Following the Python package `interpretml` [46], which we use in this study, we refer to this method as EGBM.

EGBM follows a two-stage construction approach [39], learning the main effects first and the interaction effects second. We initialise the prediction at constant  $\beta_0$  in Step 1 of Algorithm 3. After  $m \in \{1, \dots, M\}$  iterations, the univariate function describing the main effect of feature  $k \in \{1, \dots, \eta\}$  is denoted  $f_k^m$ . It is learned with gradient boosting using only feature  $k$  in a tree stump, cycling through the features. This is detailed in Steps 2–7 of Algorithm 3. For the  $k$ th main effect at iteration  $m$ , we evaluate gradients at the most recent prediction function, which is defined as

$$f_k^{m*}(\mathbf{x}) = \begin{cases} \beta_0 + \sum_{j=1}^{\eta} f_j^{m-1}(x_j), & k = 1 \\ \beta_0 + \sum_{j=1}^{k-1} f_j^m(x_j) + \sum_{j=k}^{\eta} f_j^{m-1}(x_j), & k > 1. \end{cases}$$



Note that the prediction function  $f_k^{m*}$  takes the vector of covariates  $\mathbf{x}$  as an argument while the main effect  $f_k^m$  takes only the scalar  $x_k$ .

The FAST method of [39] allows for the selection of the set  $\mathcal{S} = \{\mathbf{s}_1, \dots, \mathbf{s}_{n_{\text{int}}}\}$  containing index couples of relevant two-way interactions. This method relies on the idea that an interaction should be included if it can notably reduce the loss of the main effect model. In the second construction stage (Steps 9–14 of Algorithm 3), the interaction effect  $\tilde{f}_\ell^m$  for pair  $\mathbf{s}_\ell \in \mathcal{S}$  is learned by cycling through  $\ell \in \{1, \dots, n_{\text{int}}\}$ . The interaction is built on top of the final prediction from the main effects using trees of depth  $d = 2$ . To this end, in iteration  $m \in \{1, \dots, M\}$ , we note the most recent prediction function for the  $\ell$ th interaction effect for pair  $\mathbf{s}_\ell = (k, l)$ , that is, between  $\mathbf{x}_{\mathbf{s}_\ell} = (x_k, x_l)$ , as

$$\tilde{f}_\ell^{m*}(\mathbf{x}) = \begin{cases} \beta_0 + \sum_{j=1}^{\eta} f_j^M(x_j) + \sum_{j=1}^{n_{\text{int}}} \tilde{f}_j^{m-1}(\mathbf{x}_{\mathbf{s}_j}), & \ell = 1 \\ \beta_0 + \sum_{j=1}^{\eta} f_j^M(x_j) + \sum_{j=1}^{\ell-1} \tilde{f}_j^m(\mathbf{x}_{\mathbf{s}_j}) + \sum_{j=\ell}^{n_{\text{int}}} \tilde{f}_j^{m-1}(\mathbf{x}_{\mathbf{s}_j}), & \ell > 1. \end{cases}$$

Akin to a GAM, the equation of the EGBM prediction function is

$$\varphi\{f_{\text{EGBM}}(\mathbf{x})\} = \beta_0 + \sum_{k=1}^{\eta} f_k^M(x_k) + \sum_{\ell=1}^{n_{\text{int}}} \tilde{f}_\ell^M(\mathbf{x}_{\mathbf{s}_\ell}).$$

There is a predictor function, called shape function in [38], for each variable and for each selected interaction; gradient boosting replaces the splines used in [63]. Shape functions can be visualised and written explicitly as a formula or in a lookup table, making EGBM fully interpretable.

---

**Algorithm 3:** Explainable gradient boosting machine

---

**Inputs :**  $\mathcal{L}, \varphi, \mathcal{D}, \lambda, M$ , and  $n_{\text{int}}$ .

- 1 Initialise  $\beta_0 = \operatorname{argmin}_b \sum_{i=1}^n \mathcal{L}(y_i, b)$ .
  - 2 **for**  $m = 1$  **to**  $M$  **do**
  - 3     **for**  $k = 1$  **to**  $\eta$  **do**
  - 4         Compute  $g_i$  with Eq. (1) using  $b = f_k^{m*}(\mathbf{x}_i)$  for  $i \in \mathcal{D}$ .
  - 5         Fit tree of depth 1 to  $\{(x_{k,i}, g_i) : i \in \mathcal{D}\}$  to get regions  $R_{1,k}^m$  and  $R_{2,k}^m$ .
  - 6         Compute, for  $j \in \{1, 2\}$ ,
  - $$\hat{b}_{j,k}^m = \operatorname{argmin}_b \sum_{i \in \mathcal{D}: x_{k,i} \in R_{j,k}^m} \mathcal{L}\{y_i, f_k^{m*}(\mathbf{x}_i) + b\}.$$
  - 7         Update  $f_k^m(x_k) = f_k^{m-1}(x_k) + \lambda \sum_{j=1}^2 \hat{b}_{j,k}^m \mathbf{1}(x_k \in R_{j,k}^m)$ .
  - 8 Select  $n_{\text{int}}$  interactions with the FAST method [39] and get  $\mathcal{S}$ .
  - 9 **for**  $m = 1$  **to**  $M$  **do**
  - 10     **for**  $\ell = 1$  **to**  $n_{\text{int}}$  **do**
  - 11         Compute  $g_i$  with Eq. (1) using  $b = \tilde{f}_\ell^{m*}(\mathbf{x}_i)$  for  $i \in \mathcal{D}$ .
  - 12         Fit tree of depth 2 to  $\{(\mathbf{x}_{\mathbf{s}_\ell, i}, g_i) : i \in \mathcal{D}\}$  to get regions  $\tilde{R}_{1,\ell}^m$  and  $\tilde{R}_{2,\ell}^m$ .
  - 13         Compute, for  $j \in \{1, 2\}$ ,
  - $$\tilde{b}_{j,\ell}^m = \operatorname{argmin}_b \sum_{i \in \mathcal{D}: \mathbf{x}_{\mathbf{s}_\ell, i} \in \tilde{R}_{j,\ell}^m} \mathcal{L}\{y_i, \tilde{f}_\ell^{m*}(\mathbf{x}_i) + b\}.$$
  - 14         Update  $\tilde{f}_\ell^m(\mathbf{x}_{\mathbf{s}_\ell}) = \tilde{f}_\ell^{m-1}(\mathbf{x}_{\mathbf{s}_\ell}) + \lambda \sum_{j=1}^2 \tilde{b}_{j,\ell}^m \mathbf{1}(\mathbf{x}_{\mathbf{s}_\ell} \in \tilde{R}_{j,\ell}^m)$ .
  - 15 Aggregate  $f^M(\mathbf{x}) = \beta_0 + \sum_{k=1}^{\eta} f_k^M(x_k) + \sum_{\ell=1}^{n_{\text{int}}} \tilde{f}_\ell^M(\mathbf{x}_{\mathbf{s}_\ell})$ .
  - 16 **Return :** Prediction function  $f_{\text{EGBM}}(\mathbf{x}) \leftarrow \varphi^{-1}\{f^M(\mathbf{x})\}$ .
-

## 3.2 Probabilistic gradient boosting for decision trees

In Fig. 1, recently developed GBDT algorithms tackle the prediction of a probability distribution given  $\mathbf{x}$ . Most probabilistic GBDT approaches, such as XGBoostLSS, cyc-GBM, and NGBoost, aim to predict all the parameters of an assumed distribution. A different approach is proposed in [58]: probabilistic gradient boosting machine (PGBM) outputs the mean and variance of the target variable for fixed  $\mathbf{x}$  by treating  $g_i$ ,  $t_i$ , and  $\hat{b}_j^m$  from Eq. (3) as random variables. Thus, PGBM is a nonparametric approach limited to location-scale distributional families, which excludes, e.g., the gamma. For this reason, we focus on multi-parametric probabilistic GBDT algorithms, which use  $\kappa$  sequences of trees, one per element of  $\mathbf{p} = (p_1, \dots, p_\kappa)$ , the vector parametrizing the assumed distribution. In this section, we detail the algorithms of XGBoostLSS [41], cyc-GBM [11], and NGBoost [16].

### 3.2.1 XGBoostLSS

XGBoostLSS [41] extends the principles of gamboostLSS [33] to GBDT by joining the flexibility of GAMLSS [52] and the scalability of XGBoost [6]. It is designed as a “wrapper around XGBoost” [41]. We use the negative log-likelihood of the assumed distribution as objective  $\mathcal{L}$  and its first two partial derivatives w.r.t. each element of  $\mathbf{p}$ .

Algorithm 4 presents XGBoostLSS, as introduced in [41], with our notation. We initialise each parameter estimate with MLE and allow for different link functions  $\varphi_1, \dots, \varphi_\kappa$ . A sequence of  $M$  boosting iterations is made on each element  $k \in \{1, \dots, \kappa\}$  of  $\mathbf{p}$ . In each cycle, the XGBoost iterations update the  $k$ th prediction function while treating the other parameters fixed. In cycle  $q \in \{0, \dots, q_{\max}\}$ , when updating parameter  $k$  at iteration  $m \in \{1, \dots, M\}$ , we define the previous step vector of prediction functions as  $\hat{\mathbf{p}}_{k,q}^{m*}(\mathbf{x}_i) = \{\hat{p}_{k,q,1}^{m*}(\mathbf{x}), \dots, \hat{p}_{k,q,\kappa}^{m*}(\mathbf{x})\}$  with  $j$ th element

$$\hat{p}_{k,q,j}^{m*}(\mathbf{x}) = \begin{cases} f_{j,0}^0(\mathbf{x}), & q = 0, k \neq j, \\ f_{j,q}^{m-1}(\mathbf{x}), & q \geq 0, k = j, \\ f_{j,q-1}^M(\mathbf{x}), & q > 0, k < j, \\ f_{j,q}^M(\mathbf{x}), & q > 0, k > j. \end{cases}$$

For the first cycle, i.e., when  $q = 0$ , the elements of  $\mathbf{p}$  that are not currently being updated do not depend on  $\mathbf{x}$ : their initial values are used. In subsequent cycles, we evaluate at the most recent prediction function. We

---

#### Algorithm 4: XGBoostLSS

---

**Inputs :** Negative log-likelihood  $\mathcal{L}$ ,  $\varphi_1, \dots, \varphi_\kappa$ ,  $\mathcal{D}$ ,  $\delta$ ,  $\zeta$ ,  $\lambda$ ,  $d$ ,  $M$ ,  $\gamma$ ,  $\phi$ , and  $q_{\max}$ .

- 1 Initialise  $q = 0$  and  $\mathbf{f}_q^0(\mathbf{x}) = \{f_{1,q}^0(\mathbf{x}), \dots, f_{\kappa,q}^0(\mathbf{x})\} = \operatorname{argmin}_{\mathbf{p}} \sum_{i=1}^n \mathcal{L}(y_i, \mathbf{p}) \quad \forall q$ .
- 2 **for**  $k = 1$  **to**  $\kappa$  **do**
- 3     **for**  $m = 1$  **to**  $M$  **do**
- 4         Sample  $\mathcal{D}'$ , a subset of  $\delta n$  observations without replacement from  $\mathcal{D}$ .
- 5         Compute  $g_{i,k} = \frac{-\partial \mathcal{L}(y_i, \mathbf{p})}{\partial p_k}$  and  $t_{i,k} = \frac{-\partial^2 \mathcal{L}(y_i, \mathbf{p})}{\partial p_k^2}$  with  $\mathbf{p} = \hat{\mathbf{p}}_{k,q}^{m*}(\mathbf{x}_i)$  for  $i \in \mathcal{D}'$ .
- 6         Do Steps 5 and 6 of Algorithm 2 using  $g_{i,k}$  and  $t_{i,k}$  in place of  $g_i$  and  $t_i$ .
- 7         Update  $f_{k,q}^m(\mathbf{x}) = f_{k,q}^{m-1}(\mathbf{x}) + \lambda \sum_{j=1}^{J_{m,k}} \hat{b}_{j,k}^m \mathbf{1}(\mathbf{x} \in R_{j,k}^m)$ .
- 8 **while**  $\mathcal{L}$  has not converged and  $q \leq q_{\max}$  **do**
- 9     Increment  $q = q + 1$ .
- 10    **for**  $k = 1$  **to**  $\kappa$  **do**
- 11       Update  $f_{k,q}^M(\mathbf{x})$  by executing Steps 3 to 7.
- 12 **Return :** Vector of prediction functions

$$\mathbf{f}_{\text{XGBoostLSS}}(\mathbf{x}) = [\varphi_1^{-1}\{f_{1,q}^M(\mathbf{x})\}, \dots, \varphi_\kappa^{-1}\{f_{\kappa,q}^M(\mathbf{x})\}].$$


---



cycle until convergence of  $\mathcal{L}$  with pre-specified tolerance or until the process has been repeated ( $q_{\max} + 1$ ) times. The output is a vector of  $\kappa$  prediction functions for distributional parameters given  $\mathbf{x}$ .

### 3.2.2 Cyclic gradient boosting machine

A different approach to probabilistic GBDT is advocated in [11]: cyc-GBM, a framework unifying multi-parametric boosting algorithms that use cyclic gradient descent. It includes the dual-parameter boosting of [45]. In cyclic coordinate descent [see, e.g., Section 8.8 of 40], distributional parameters are successively updated within each boosting iteration. Training time should be greater for cyc-GBM than for XGBoostLSS: cyclic gradient descent is more computationally intensive than Newton steps. The cyc-GBM algorithm relies on GBM, so optimisation is needed in each iteration.

Algorithm 5 presents the cyc-GBM algorithm of [11] in our notation. When updating parameter  $k \in \{1, \dots, \kappa\}$  in iteration  $m \in \{1, \dots, M_k\}$ , the previous step vector of prediction functions is  $\hat{\mathbf{p}}_k^{m*}(\mathbf{x}) = \{\hat{p}_{k,1}^{m*}(\mathbf{x}), \dots, \hat{p}_{k,\kappa}^{m*}(\mathbf{x})\}$ , with  $j$ th element

$$\hat{p}_{k,j}^{m*}(\mathbf{x}) = \begin{cases} f_j^0(\mathbf{x}), & k \geq 1, m = 1, k \leq j, \\ f_j^{m-1}(\mathbf{x}), & k \geq 1, m > 1, k \leq j, \\ f_j^m(\mathbf{x}), & k > 1, m \geq 1, k > j. \end{cases}$$

The cyc-GBM algorithm [11] is designed to enhance flexibility in multi-parametric GBDT. Different tree depth, learning rate, and number of trees per distributional parameter are allowed in cyc-GBM. This feature may prevent overfitting on some distributional parameters while others are still undertrained. For enhanced explainability, we can set  $d_k = 0$  for some  $k$  if, e.g., when we do not want a parameter to vary with  $\mathbf{x}$ .

---

#### Algorithm 5: Cyclic gradient boosting machine

---

**Inputs :** Negative log-likelihood  $\mathcal{L}, \varphi_1, \dots, \varphi_\kappa, \mathcal{D}, \lambda_1, \dots, \lambda_\kappa, d_1, \dots, d_\kappa$ , and  $M_1, \dots, M_\kappa$ .

- 1 Initialise  $\mathbf{f}^0(\mathbf{x}) = \{f_1^0(\mathbf{x}), \dots, f_\kappa^0(\mathbf{x})\} = \operatorname{argmin}_{\mathbf{p}} \sum_{i=1}^n \mathcal{L}(y_i, \mathbf{p})$
- 2 **for**  $m = 1$  **to**  $M = \max(M_1, \dots, M_\kappa)$  **do**
- 3     **for**  $k = 1$  **to**  $\kappa$  **do**
- 4         Fix  $\mathbf{u}_k$ , a unit (vertical) vector of length  $\kappa$  with a 1 in the  $k$ th position.
- 5         **if**  $m \leq M_k$  **then**
- 6             Compute  $g_{i,k} = -\left. \frac{\partial \mathcal{L}(y_i, \mathbf{p})}{\partial p_k} \right|_{\mathbf{p}=\hat{\mathbf{p}}_k^{m*}(\mathbf{x}_i)}$ , for  $i \in \mathcal{D}$ .
- 7             Fit tree of depth  $d_k$  to  $\{(\mathbf{x}_i, g_{i,k}) : i \in \mathcal{D}\}$  to get terminal regions  $R_{1,k}^m, \dots, R_{J_{m,k},k}^m$ .
- 8             For  $j \in \{1, \dots, J_{m,k}\}$ , compute
 
$$\hat{b}_{j,k}^m = \operatorname{argmin}_b \sum_{i:\mathbf{x}_i \in R_{j,k}^m} \mathcal{L}\{y_i, \hat{\mathbf{p}}_k^{m*}(\mathbf{x}_i) + \mathbf{u}_k b\}.$$
- 9             Update  $f_k^m(\mathbf{x}) = f_k^{m-1}(\mathbf{x}) + \lambda \sum_{j=1}^{J_{m,k}} \hat{b}_{j,k}^m \mathbf{1}(\mathbf{x} \in R_{j,k}^m)$ .
- 10         **else** Set  $f_k^m(\mathbf{x}) = f_k^{m-1}(\mathbf{x})$ .
- 11 **Return :** Vector of prediction functions

$$\mathbf{f}_{\text{cyc-GBM}}(\mathbf{x}) = [\varphi_1^{-1}\{f_1^M(\mathbf{x})\}, \dots, \varphi_\kappa^{-1}\{f_\kappa^M(\mathbf{x})\}].$$


---

### 3.2.3 Natural gradient boosting

In XGBoostLSS and cyc-GBM, it is not true in general that the change indicated by the computed gradients  $g_{i,k}$  corresponds to an equivalent change in probability space. As explained in [16], “[t]he problem

is that ‘distance’ between two parameter values does not correspond to an appropriate ‘distance’ between the distributions that those parameters identify.” This motivates the use of the natural gradient in the multi-parameter GBDT approach named NGBost [16]. While the classical gradient  $\nabla\mathcal{L}(y, \mathbf{p})$  lacks the property of invariance under reparametrisation, an invariant alternative is the generalized natural gradient, defined as

$$\tilde{\nabla}\mathcal{L}(y, \mathbf{p}) \propto \mathcal{I}_{\mathcal{L}}^{-1}(\mathbf{p})\nabla\mathcal{L}(y, \mathbf{p}),$$

where  $\mathcal{I}_{\mathcal{L}} = \mathbb{E}[\nabla\mathcal{L}(Y, \mathbf{p})\nabla\mathcal{L}(Y, \mathbf{p})^\top]$ , the Fisher information matrix because the loss function is the negative log-likelihood. The disadvantage of the natural gradient is that its evaluation requires the inversion of a  $\kappa \times \kappa$  matrix. In NGBost, we need to invert this matrix for each training observation at each iteration.

**Remark 3.** *The natural gradient can be generalized to the use of any proper scoring rule as a loss function. We refer to [16] for the technical details.*

Algorithm 6 is the NGBost procedure of [16] in our notation. This algorithm is very close to a vectorized version of Algorithm 1. In each iteration of NGBost,  $\kappa$  trees are built in Step 4. The vector of tree predictions  $\mathbf{h}^m(\mathbf{x})$  is scaled with a scalar factor  $\hat{\rho}^m$ , optimized globally in Step 5, before being added to the vector of prediction functions in the update of Step 6. Interestingly, the prediction of the decision tree participates directly to the NGBost prediction function: in other GBDT algorithms, the update depends on the tree only through terminal regions. Also, unlike in XGBostLSS and cyc-GBM, all parameter prediction functions are updated simultaneously. As hinted in [16], NGBost could predict multivariate responses with a joint log-likelihood. We use the R wrapper `ngboostR` [4] in this study.

---

**Algorithm 6:** Natural gradient boosting

---

**Inputs :** Negative log-likelihood  $\mathcal{L}$ ,  $\varphi_1, \dots, \varphi_\kappa$ ,  $\mathcal{D}$ ,  $\lambda$ ,  $d$ , and  $M$ .

1 Initialise  $\mathbf{f}^0(\mathbf{x}) = \operatorname{argmin}_{\mathbf{p}} \sum_{i=1}^n \mathcal{L}(y_i, \mathbf{p})$ .

2 **for**  $m = 1$  **to**  $M$  **do**

3     Compute  $\mathbf{g}_i = \tilde{\nabla}\mathcal{L}(y, \mathbf{p})|_{\mathbf{p}=\mathbf{f}^{m-1}(\mathbf{x}_i)}$ , for  $i \in \mathcal{D}$ .

4     **for**  $k = 1$  **to**  $\kappa$ , fit tree of depth  $d$  to  $\{(\mathbf{x}_i, g_{i,k}) : i \in \mathcal{D}\}$  to get predictor  $h_k^m(\mathbf{x})$ .

5     Optimise, by denoting  $\mathbf{h}^m(\mathbf{x}) = \{h_1^m(\mathbf{x}), \dots, h_\kappa^m(\mathbf{x})\}$ ,

$$\hat{\rho}^m = \operatorname{argmin}_{\rho} \sum_{i=1}^n \mathcal{L}\{y_i, \mathbf{f}^{m-1}(\mathbf{x}_i) + \rho\mathbf{h}^m(\mathbf{x}_i)\}.$$

6     Update  $\mathbf{f}^m(\mathbf{x}) = \mathbf{f}^{m-1}(\mathbf{x}) + \lambda\hat{\rho}^m\mathbf{h}^m(\mathbf{x})$ .

7 **Return :** Vector of prediction functions

$$\mathbf{f}_{\text{NGBost}}(\mathbf{x}) = [\varphi_1^{-1}\{f_1^M(\mathbf{x})\}, \dots, \varphi_\kappa^{-1}\{f_\kappa^M(\mathbf{x})\}].$$


---

### 3.3 Algorithmic hybridisation

The algorithms presented in this section correspond to the nodes in Fig. 1. To the best of our knowledge, this is a comprehensive survey of the existing point and multi-parametric probabilistic GBDT algorithms in literature. However, creating hybrid algorithms is possible. For example, the DART procedure can always replace shrinkage.

Examples of algorithmic hybrids are CatBoostLSS [42] and LightGBMLSS [43] which replace XGBost by CatBoost or LightGBM to sequentially estimate distributional parameters following Algorithm 4. The DART algorithm is used in [45] to perform dual-parameter boosting for claim frequency modelling with a zero-inflated Poisson and a negative binomial distribution. We use the DART along with XGBostLSS

instead of shrinkage, which we denote XGBoostLSSd. The natural gradient, as in NGBoost, is coupled with LightGBM to predict the cost of novel constructions in [5]. Finally, any GBDT prediction algorithm can leverage shallow trees and selected two-way interactions as in EGBM to enhance model interpretability. The possibilities are numerous; we focus on comparing the native algorithms in our numerical experiment.

## 4 Methods

Our objective is to compare the performance of the algorithms presented in Section 3 on actuarial data. Distributional assumptions for claim frequency and severity are set in Section 4.1 with a special emphasis on the treatment of varying exposure-to-risk. Then, we present the metrics for computational time, predictive performance, and model adequacy in Section 4.2. Appendix A details training and tuning strategies.

### 4.1 Distributional assumptions for claim frequency and severity

We consider the modelling of insurance claim frequency, with the Poisson and negative binomial distributions, and severity, with the lognormal and gamma distributions.

Within an insurance portfolio, each policy  $i \in \{1, \dots, n\}$  is observed for a given duration  $e_i$ . Claim frequency modelling should take into account varying exposure-to-risk. In a Poisson GLM with log link, this is classically treated by an offset term  $\ln e_i$ . We adopt this idea in the GBDT framework. The initial prediction for the claim frequency of policy  $i$  is  $\ln e_i + \ln f^0(\mathbf{x}_i)$ , which is refined with boosting iterations. The offset  $\ln e_i$  is introduced in GBDT implementations with the argument called *initial\_score*, *baseline* or *base score* depending on the package.

Because insurance claim data is often overdispersed, we also consider the negative binomial distribution. The NB2 distribution with probability mass function

$$f(y_i) = \frac{\Gamma(\phi_i + y_i)}{\Gamma(\phi_i)\Gamma(y_i + 1)} \left(\frac{\mu_i}{\mu_i + \phi_i}\right)^{y_i} \left(\frac{\phi_i}{\mu_i + \phi_i}\right)^{\phi_i}$$

is conveniently parametrized by a location parameter  $\mu$  and a dispersion parameter  $\phi$ . This parametrization allows to treat varying exposure-to-risk as an offset for parameter  $\mu_i$  while treating  $\phi_i$  without the exposure-to-risk. The principles of Section 2 apply: dispersion parameter  $\phi_i$  can be estimated either individually through a multi-parametric GBDT algorithm or globally ( $\phi_i = \phi \forall i$ ) with MLE after learning the prediction function for  $\mu_i$ , e.g. with the MASS package [62].

For the lognormal assumption on claim severity, we use  $\ln Y$  as the target with a normal distribution and the squared error loss function. For convenience, we parametrize the gamma distribution with mean  $\mu$  and shape  $\alpha$ .

**Remark 4.** *Approaches that directly model the loss cost with a Tweedie distribution are implemented, for example, with GBM in [12]. The Tweedie loss function is readily available in packages `gbm3`, `xgboost`, `lightgbm`, `catboost`, `interpretml`, and `pgbm`.*

### 4.2 Performance metrics

We measure computational efficiency by the training time in seconds on a personal laptop computer (IntelCore i7-1195G7 @ 2.90 GHz CPU) for a fixed combination of hyperparameters ( $M = 800$ ,  $d = 5$ ,  $\delta = 0.75$ , and  $\lambda = 0.01$ ), common to all the algorithms. This way, we compare the difference induced by the operations of each algorithm for a comparable configuration without regards to tuning.

As evoked in Section 2, we use the deviance to measure predictive performance. With negative log-likelihood  $\mathcal{L}$ , the deviance of observation  $i \in \{1, \dots, n\}$  is

$$D\{y_i, f_{\text{GBDT}}(\mathbf{x}_i)\} = 2[-\mathcal{L}(y_i, y_i) + \mathcal{L}\{y_i, f_{\text{GBDT}}(\mathbf{x}_i)\}].$$

Although the deviance measures the predictive performance of  $f_{\text{GBDT}}$ , its absolute value does not have an inherent meaning or scale. Inspired by [56], we thus present an alternative predictive performance metric

named McFadden’s pseudo- $R^2$ , which measures the improvement in predictive performance compared to the constant  $\bar{y}$  model [44]. For a test set of  $n_{test}$  observations, the expression is

$$R^2 = 1 - \frac{\sum_{i=1}^{n_{test}} D\{y_i, f_{GBDT}(\mathbf{x}_i)\}}{\sum_{i=1}^{n_{test}} D(y_i, \bar{y})}.$$

A model is better if its McFadden’s pseudo- $R^2$  is closer to one.

Model adequacy informs on how well an estimated assumed distribution fits the data. In particular, a model is inadequate if some observations are highly unlikely given the estimated parameters. We quantify model adequacy with proper scoring rules, functions that assign a score to a probabilistic prediction given the corresponding observation. Smaller values of proper scoring rules indicate better model adequacy [see, e.g, 26]. For an estimated cumulative distribution function  $F_{\hat{\mathbf{p}}}$ , the continuous ranked probability score (CRPS) is given by

$$CRPS(F_{\hat{\mathbf{p}}}, y_i) = \int_{-\infty}^{\infty} \{F_{\hat{\mathbf{p}}}(z) - \mathbf{1}(y_i \leq z)\}^2 dz.$$

The R package `scoringRules` [34] implements the CRPS. With frequency data, we use double probability integral transform (DPIT) residuals [68], which should follow a uniform distribution when the model is adequate.

To measure the adequacy of continuous distributions to severity data, we also look at the coverage of confidence intervals (CIs) on the test set. In this context, the probabilistic forecast of an observation leads to an estimated distribution function from which we can compute CIs. The proportion of observations in the test set that fall inside their corresponding predicted CI is the coverage. In an adequate model, CI coverage is near CI level. In Fig. 2, the observed response drawn with a black vertical line falls within the 95% CIs predicted by NGBost and XGBoostLSS (blue and green vertical lines). However, the XGBoost model (pink) does not fit well this observation.

Here, we compare the competing algorithms under a given distribution family assumption. It differs from the usual setup, where the competing distributions obtained with a given algorithm are compared.

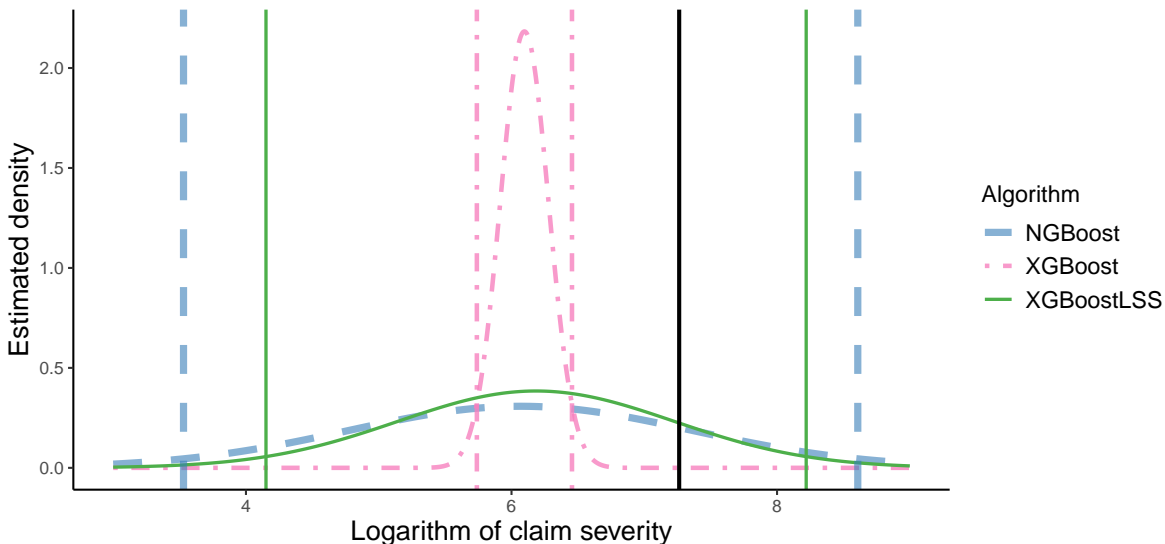


Figure 2: Predicted lognormal densities given  $\mathbf{x}_1$  by three algorithms (color and line type), corresponding 95% confidence intervals, and target  $y_1$  (black bold vertical line).

Table 1: Characteristics of the claim frequency datasets.

Name	Preprocessing	Sample size	# of features	# of cat. variables	Max. # of levels for cat. variables
freMTPL	[56]	678 013	9	4	21
freMPL	[30]	165 200	9	6	46
BelgianMTPL	[31]	163 212	11	5	3
swauto	[47]	62 436	6	4	7
pg15training9	[66]	50 000	13	8	471

Table 2: Characteristics of the claim severity datasets.

Name	Preprocessing	Sample size	# of features	# of cat. variables	Max. # of levels for cat. variables
WorkComp		48 703	21	3	3
freMTPL	[56]	21 611	9	4	21
BelgianMTPL	[31]	17 910	11	5	3
pg15training	[66]	12 256	14	9	471
Emcien		9 134	17	12	9

## 5 Results

Performances of the point and probabilistic GBDT algorithms in Fig. 1 are compared within the same experimental setup on various publicly available datasets.

The characteristics of the publicly available datasets used for frequency modelling are presented in Table 1. All of them are non-synthetic and include a column for the exposure  $e_i$ . The diversity in sample size, number of features, number of categorical variables, and maximum number of levels for categorical variables allows to assess the influence of these characteristics on performances. In Table 1, we list which source inspired the preprocessing. Note that, for pg15training, we only use the 2009 cohort for claim frequency modelling. We present the datasets for severity modelling in Table 2. Most datasets are from CASDatasets [17]; BelgianMTPL is introduced in [14], Emcien can be found in [19], and the synthetic WorkComp data in [49].

We preprocess data and compute results with R. However, the Python implementations of EGBM, XGBoostLSS, and cyc-GBM are used because there is no equivalent in R. We present results on computational efficiency in Section 5.1 and predictive performance in Section 5.2. In Section 5.3, we analyse model adequacy.

### 5.1 Computational efficiency

The results on computational efficiency for the Poisson and NB2 frequency models are presented in Tables 3 and 4, respectively. The horizontal line delimits the point and probabilistic algorithms; we provide the average ranking over all datasets within each type of algorithm in the last column. LightGBM and XGBoostLSS stand out in their category as the most computationally efficient. Other key takeaways of Tables 3–4 are:

- The major gap between training time for XGBoostLSS with shrinkage and with DART illustrates that the latter is time-consuming.
- Predicting the dispersion parameter in addition to the location parameter for the NB2 distribution more than doubles the training time in most of the cases.
- Sample size (decreasing from left to right in the tables) and the number of levels in categorical features impact training time. The comparison between freMPL and BelgianMTPL illustrates the influence of the cardinality of categorical variables.
- XGBoost and LightGBM have smaller training times than GBM, as expected.

Table 3: Training time in seconds for Poisson frequency models.

Model	Dataset					Avg. rank
	freMTPL	freMPL	BelgianMTPL	swauto	pg15training	
LightGBM	20	6	7	3	6	1.0
XGBoost	1 120	38	34	22	13	2.4
EGBM	1 015	481	82	15	49	3.4
GBM	3 829	50	38	24	17	3.6
CatBoost	1 780	106	84	34	51	4.6
XGBoostLSS	1 153	38	35	24	15	1.0
NGBoost	4 653	361	223	65	145	2.0
cyc-GBM	9 313	452	349	136	238	3.2
XGBoostLSSd	10 341	757	264	414	377	3.8

Table 4: Training time in seconds for NB2 frequency models.

Model	Dataset					Avg. rank
	freMTPL	freMPL	BelgianMTPL	swauto	pg15training	
XGBoostLSS	3 248	112	60	75	55	1.0
NGBoost	8 532	1 100	424	101	252	2.0
cyc-GBM	16 034	2 646	948	705	863	3.4
XGBoostLSSd	17 360	2 833	514	805	731	3.6

Table 10 in Appendix B displays the training time for lognormal models and lead to similar takeaways. Results for PGBM and XGBoost are similar because the same algorithm is used; training times are slightly higher in PGBM due to the estimation of variances in each terminal tree node. Similar conclusions were obtained with the gamma distribution (not shown).

## 5.2 Predictive performance

Tables 5–8 show McFadden’s  $R^2$  for the Poisson, NB2, lognormal, and gamma models, respectively. The last column is the average ranking over all datasets and models. Algorithms are ordered following the computational efficiency average ranks: lower entries take longer to train on average. Note that, in a Poisson model, point and probabilistic predictions are equivalent.

For a given dataset, the magnitude of the  $R^2$  is broadly the same for all algorithms: probabilistic forecasting does not hinder much predictive performance. This is also seen in the average ranking, which is not as clear as in the computational efficiency comparison. In terms of average rank, CatBoost wins, whereas cyc-GBM loses, in three of the four tables. The specific design of CatBoost seems advantageous, especially for datasets with high cardinality categorical features, commonly seen in actuarial pricing. Interestingly, EGBM has a slightly better performance than GBM while being fully interpretable. Also, XGBoostLSS performs better with DART rather than shrinkage on all frequency datasets but swauto at the cost of an increased training time (see Section 5.1). This is not observed in severity models. Finally, the relative ordering of LightGBM, XGBoost, and CatBoost with freMTPL on Poisson boosting is consistent with results in [56].

Table 5: McFadden’s pseudo- $R^2$  of test Poisson deviance (in %).

Model	Dataset					Avg. rank
	freMTPL	freMPL	BelgianMTPL	swauto	pg15training	
LightGBM	<b>24.92</b>	65.86	4.52	<b>26.31</b>	22.79	3.6
XGBoost	24.87	66.68	4.45	24.81	22.42	5.6
EGBM	23.92	65.99	<b>4.64</b>	25.97	24.95	3.4
GBM	23.85	65.14	4.63	26.03	24.11	4.4
CatBoost	24.91	65.67	4.56	26.25	<b>24.99</b>	2.8
XGBoostLSS	24.84	66.77	4.39	24.92	21.39	5.6
NGBoost	22.87	62.42	4.31	24.56	23.61	7.2
cyc-GBM	16.85	60.16	3.93	21.49	22.88	8.4
XGBoostLSSd	24.90	<b>66.94</b>	4.48	24.83	22.98	4.0

Table 6: McFadden’s pseudo- $R^2$  of test negative binomial deviance (in %).

Model	Dataset					Avg. rank
	freMTPL	freMPL	BelgianMTPL	swauto	pg15training	
XGBoostLSS	20.84	61.29	1.71	<b>25.02</b>	11.80	2.6
NGBoost	<b>22.56</b>	61.84	1.48	24.98	12.61	2.2
cyc-GBM	12.49	54.72	<b>3.62</b>	21.91	10.82	3.4
XGBoostLSSd	22.16	<b>62.77</b>	2.69	23.11	<b>13.30</b>	1.8

Table 7: McFadden’s pseudo- $R^2$  on the test set based on RMSE for the lognormal models (in %).

Model	Dataset					Avg. rank
	WorkComp	freMTPL	BelgianMTPL	pg15training	Emcien	
LightGBM	<b>29.83</b>	0.71	0.44	0.34	49.07	5.8
XGBoost	29.03	0.81	<b>0.51</b>	1.22	48.89	4.0
EGBM	29.59	0.76	0.45	1.52	48.85	5.1
GBM	26.27	0.78	0.48	0.60	48.89	6.5
CatBoost	24.11	<b>0.83</b>	0.50	<b>1.52</b>	<b>50.89</b>	3.2
PGBM	29.01	0.80	0.50	1.20	48.86	5.3
XGBoostLSS	29.82	0.75	-0.33	1.31	48.93	5.1
NGBoost	29.39	0.78	0.48	1.22	48.93	4.6
cyc-GBM	29.53	0.18	-0.50	0.85	48.39	8.4
XGBoostLSSd	29.82	0.75	0.23	0.76	48.72	7.0

### 5.3 Model Adequacy

Table 9 shows the average rank in CRPS (lower is better) for the Poisson, NB2, lognormal, and gamma models. For the frequency models, we report the uniform CRPS of the DPIT residuals. We show the values of CRPS in Tables 11–14 of Appendix B.

The Poisson distribution taking only a mean parameter, probabilistic and point predictions are equivalent, which leads to no clear distinction between the algorithms in terms of average rank in Table 9. With the NB2 distribution, probabilistic prediction algorithms are, on average, less adequate than point prediction algorithms in Table 9. This suggests that allowing the shape parameter  $\phi_i$  to vary with  $\mathbf{x}_i$  hinders model adequacy, at least on all the studied datasets (see Table 12).

With the lognormal loss in Table 9, we observe lower CRPS average ranks for probabilistic algorithms



Table 8: McFadden’s pseudo- $R^2$  on the test set based on the gamma deviance for the gamma models.

Model	Dataset					Avg. rank
	WorkComp	freMTPL	BelgianMTPL	pg15training	Emcien	
LightGBM	33.24	-0.45	0.65	3.90	68.47	6.0
XGBoost	32.14	-0.04	0.76	<b>5.56</b>	72.75	3.0
EGBM	32.94	-0.28	0.53	4.64	72.65	5.2
GBM	26.33	-0.09	0.52	1.95	72.73	6.4
CatBoost	31.47	-0.06	0.81	5.38	<b>72.85</b>	3.2
XGBoostLSS	32.72	<b>0.72</b>	0.61	5.33	72.71	3.8
NGBoost	<b>33.75</b>	-0.53	<b>0.89</b>	5.40	72.19	3.4
cyc-GBM	25.17	-7.22	0.79	4.84	71.97	6.6
XGBoostLSSd	32.19	-1.30	0.20	4.22	71.96	7.4

Table 9: Average rank of CRPS for the models under the considered distributional assumptions.

Model	Distribution			
	Poisson	NB2	Lognormal	Gamma
LightGBM	5.0	1.8	6.4	4.4
XGBoost	3.6	2.2	6.8	5.4
EGBM	7.6	5.0	7.8	5.2
GBM	7.2	4.6	8.2	8.6
CatBoost	4.2	2.8	6.6	2.6
XGBoostLSS	2.4	6.8	1.6	5.8
NGBoost	4.6	7.0	2.2	2.4
cyc-GBM	6.2	7.8	3.2	3.0
XGBoostLSSd	4.0	7.0	2.8	7.4

than for point algorithms. The latter aim to minimise the distance between predictions and the predicted location parameter, regardless of the scale, whereas probabilistic algorithms optimise both parameters. Such model adequacy difference does not manifest in gamma models because the gamma deviance optimised by point algorithms already entails both location and shape parameters.

The same dichotomy between lognormal and gamma models is diagnosed with CI coverage. Fig. 3 displays CI coverage for confidence levels 50%, 75%, and 95% (columns) on the BelgianMTPL dataset for point (light grey) and probabilistic (dark grey) algorithms with lognormal (top) and gamma (bottom). In each panel, a model is adequate if its bar approaches the vertical dashed line. Overall, gamma models are adequate, whereas CI predictions from lognormal point algorithms are too narrow to satisfyingly fit the BelgianMTPL severity data. A good improvement is obtained with probabilistic lognormal models, especially XGBoostLSS (with shrinkage and DART) and NGBoost. The values of CI coverage on all test datasets are in Tables 15–19 of Appendix B. For CatBoost on the Emcien dataset, the estimated lognormal scale parameter is so large that CI coverage is 100% at levels 75% or 95% (see Table 19).

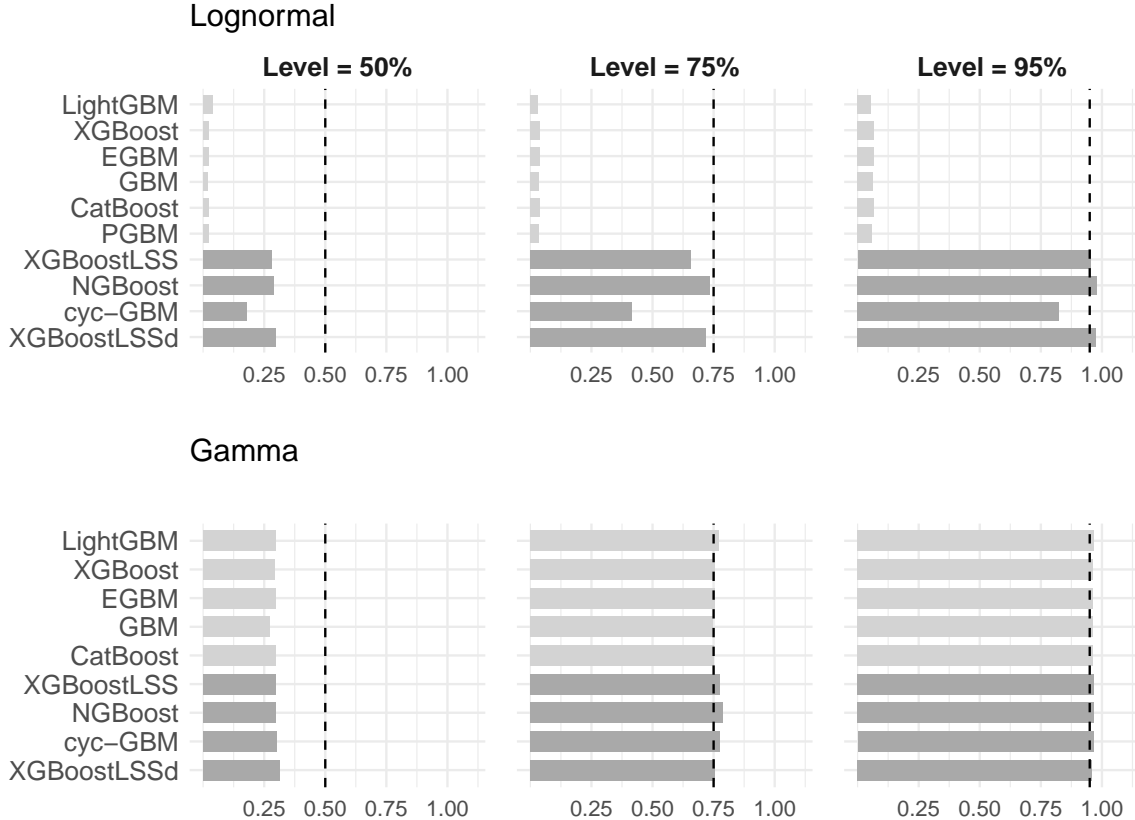


Figure 3: Coverage of CI with levels 50%, 75%, and 95% on the test BelgianMTPL set for point (light) or probabilistic (dark) prediction algorithms.

## 6 Discussion

In this study, we gather the recent developments of GBDT for point and probabilistic predictions in a unified notation. We adopt an actuarial standpoint as GBMs are considered as an alternative to GLMs in general insurance ratemaking and reserving. GBDT approaches compete on five actuarial datasets for claim frequency and severity modelling, based on computational efficiency, predictive performance and model fit.

There is no one-size-fits-all solution, but some algorithms stand out. LightGBM can more efficiently output predictions that are as precise as those of other algorithms. Also, CatBoost can improve predictive performance in the presence of high cardinality categorical variables, which are frequent in insurance. Finally, model adequacy may be enhanced by using probabilistic GBDT without hurting much predictive performance. We find that XGBoostLSS is the most computationally efficient probabilistic GBDT algorithm and has competitive performance.

In actuarial applications, model interpretability matters. Unlike GLMs, GBDT generally does not lead to interpretable models. Tools such as variable importance or a partial dependence plot (PDP) can help in explaining GBDT model outputs, as illustrated with the BelgianMTPL dataset in [31]. Modelling multiple distributional parameters based on covariates adds an additional layer of complexity, as these tools need to be applied on each of them. Moreover, warnings about PDPs are issued in [67]: with adversarial attacks, they can be “deceptive”.

The fully interpretable algorithm EGBM achieves competitive predictive performance compared to black box GBDT algorithms. It outputs regression parameters in a lookup table, allowing to retrieve feature and interaction effects. Fig. 4 shows the main effect  $f_{\text{ageph}}^M$  in the BelgianMTPL Poisson EGBM: its shape mimics the corresponding smooth GAMLSS effect in [36]. Interestingly, post-hoc adjustments can be made, allowing

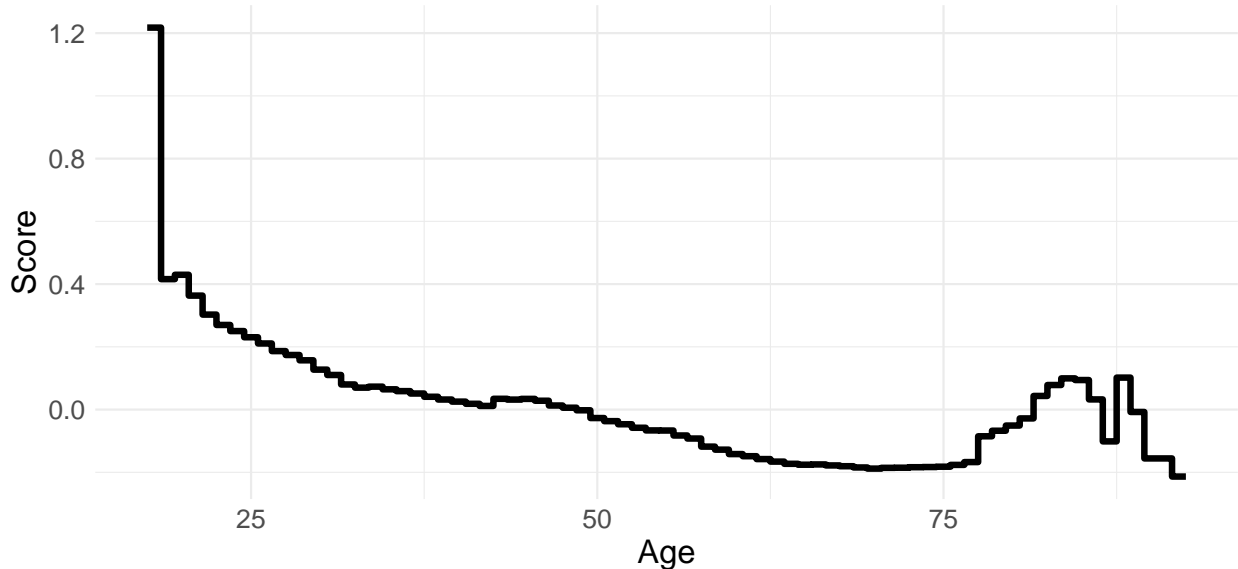


Figure 4: Main effect for the variable `ageph` in the Poisson EGBM on BelgianMTPL.

actuaries to manually handle the EGBM model’s extrapolation behaviour in rarely observed segments, e.g., when `ageph` is smaller than 20 or larger than 75 in Fig. 4. This is impossible with other opaque GBDT methods, as global or local explanations cannot be used to adjust predictions post-hoc.

Even if multi-parametric GBDT methods allow to predict a distinct value of distributional parameter per observation, it may be appropriate to keep some parameters constant. For example, an individual’s characteristics may change the behaviour of its risk, but not as dramatically as the possible variations in the shape parameter of a distribution. Under the gamma distributional assumption, we find that using a global shape parameter does not hinder much model adequacy. The shape of the gamma density is dramatically different when the shape parameter crosses one, which could indeed warrant a single shape parameter.

In NB2 models, we find that a global dispersion parameter enhances model adequacy compared to a covariate-specific dispersion parameter. One could argue that the overdispersion of a negative binomial should not vary per observation. Conceptually, overdispersion must be diagnosed with more than one observation, which could warrant to model overdispersion collectively, or over a small number of risk classes. Keeping a distributional parameter constant can be done post-hoc with point predictions (as described in Section 2) or iteratively with parameter-specific hyperparameters [as in cyc-GBM 11]: setting tree depth to zero yields a global parameter estimation.

Boosting algorithms do not have the desirable balance property of GLMs [see, e.g., 64] even if they can output probabilistic predictions. To correct this problem, an autocalibration procedure for insurance pricing is proposed in [12], and its performance with GBM is demonstrated. This procedure, along with one of the studied GBDT algorithms, could improve the adequacy of predictions for general insurance ratemaking while keeping the balance property, as  $\hat{\mu}(\mathbf{X}) = E\{Y|\hat{\mu}(\mathbf{X})\}$  is ensured by autocalibration.

## Acknowledgments

We are thankful to an anonymous insurance company for useful discussions. We acknowledge the help of Lu Yang for the implementation of DPIT residuals for Poisson models and Olivier Côté for his comments. This research was funded by the Natural Sciences and Engineering Research Council of Canada (CRDPJ 515901-17, RGPIN-2019-04190) and the Chaire d’actuariat of Université Laval.

## References

- [1] Breiman, L. (2001a). Random forests. *Machine learning*, 45:5–32.
- [2] Breiman, L. (2001b). Statistical modeling: The two cultures (with comments and a rejoinder by the author). *Statistical science*, 16(3):199–231.
- [3] Breiman, L., Friedman, J., Olshen, R., and Stone, C. (1984). *Classification and regression trees*. Taylor & Francis, New York.
- [4] Carabantes Alamo, A. (2023). *NGBoostR: R Wrapper for NGBoost python module*. R package version 0.1.8.
- [5] Chakraborty, D., Elhegazy, H., Elzarka, H., and Gutierrez, L. (2020). A novel construction cost prediction model using hybrid natural and light gradient boosting. *Advanced Engineering Informatics*, 46:101201.
- [6] Chen, T. and Guestrin, C. (2016). XGBoost: A scalable tree boosting system. *Proceedings of the 22nd ACM SIGKDD international conference on knowledge discovery and data mining*, pages 785–794.
- [7] Chen, T., He, T., Benesty, M., Khotilovich, V., Tang, Y., Cho, H., Chen, K., Mitchell, R., Cano, I., Zhou, T., Li, M., Xie, J., Lin, M., Geng, Y., Li, Y., and Yuan, J. (2023). *XGBoost: Extreme Gradient Boosting*. R package version 1.7.5.1.
- [8] Clemente, C., Guerreiro, G. R., and Bravo, J. M. (2023). Modelling motor insurance claim frequency and severity using gradient boosting. *Risks*, 11(9):163.
- [9] Crevecoeur, J., Robben, J., and Antonio, K. (2022). A hierarchical reserving model for reported non-life insurance claims. *Insurance: Mathematics and Economics*, 104:158–184.
- [10] De Jong, P. and Heller, G. Z. (2008). *Generalized linear models for insurance data*. Cambridge University Press, Cambridge.
- [11] Delong, L., Lindholm, M., and Zakrisson, H. (2023). On cyclic gradient boosting machines. *Available at SSRN 4352505*.
- [12] Denuit, M., Charpentier, A., and Trufin, J. (2021). Autocalibration and Tweedie-dominance for insurance pricing with machine learning. *Insurance: Mathematics and Economics*, 101:485–497.
- [13] Denuit, M., Hainaut, D., and Trufin, J. (2019). *Effective Statistical Learning Methods for Actuaries I: GLMs and Extensions*. Springer, Switzerland.
- [14] Denuit, M. and Lang, S. (2004). Non-life rate-making with Bayesian GAMs. *Insurance: Mathematics and Economics*, 35(3):627–647.
- [15] Dorogush, A. V., Ershov, V., and Gulin, A. (2023). *CatBoost: gradient boosting with categorical features support*. R package version 1.2.2.
- [16] Duan, T., Anand, A., Ding, D. Y., Thai, K. K., Basu, S., Ng, A., and Schuler, A. (2020). NGBoost: Natural gradient boosting for probabilistic prediction. *Proceedings of the 37th International Conference on Machine Learning*, 119:2690–2700.
- [17] Dutang, C. and Charpentier, A. (2020). *CASdatasets: Insurance datasets*. R package version 1.0-11.
- [18] Embrechts, P. and Wüthrich, M. V. (2022). Recent challenges in actuarial science. *Annual Review of Statistics and Its Application*, 9:119–140.
- [19] Emcien Patterns (2017). Automobile insurance claims including location, policy type and claim amount. Accessed 21 November 2023.
- [20] Fenske, N., Kneib, T., and Hothorn, T. (2011). Identifying risk factors for severe childhood malnutrition by boosting additive quantile regression. *Journal of the American Statistical Association*, 106(494):494–510.

- [21] Frees, E. W. (2015). Analytics of insurance markets. *Annual Review of Financial Economics*, 7(1):253–277.
- [22] Friedman, J. H. (2001). Greedy function approximation: a gradient boosting machine. *Annals of statistics*, 29:1189–1232.
- [23] Friedman, J. H. (2002). Stochastic gradient boosting. *Computational statistics & data analysis*, 38(4):367–378.
- [24] Gao, Y., Huang, Y., and Meng, S. (2023). Evaluation and interpretation of driving risks: Automobile claim frequency modeling with telematics data. *Statistical Analysis and Data Mining: The ASA Data Science Journal*, 16(2):97–119.
- [25] GDPR (2016). Regulation (EU) 2016/679 of the European Parliament and of the Council of 27 April 2016 on the protection of natural persons with regard to the processing of personal data and on the free movement of such data (general data protection regulation). *Official Journal of the European Union*, L 119:1–88. Accessed: November 11th, 2024.
- [26] Gneiting, T., Raftery, A. E., Westveld, A. H., and Goldman, T. (2005). Calibrated probabilistic forecasting using ensemble model output statistics and minimum crps estimation. *Monthly Weather Review*, 133(5):1098–1118.
- [27] Hancock, J. and Khoshgoftaar, T. M. (2020). Performance of CatBoost and XGBoost in medicare fraud detection. In *2020 19th IEEE international conference on machine learning and applications (ICMLA)*, pages 572–579.
- [28] Hartman, B., Owen, R., and Gibbs, Z. (2020). Predicting high-cost health insurance members through boosted trees and oversampling: An application using the HCCI database. *North American Actuarial Journal*, 25(1):53–61.
- [29] Hastie, T., Tibshirani, R., and Friedman, J. (2009). *The elements of statistical learning: Data mining, inference, and prediction*. Springer, New York.
- [30] Henckaerts, R., Antonio, K., and Côté, M.-P. (2022). When stakes are high: Balancing accuracy and transparency with model-agnostic interpretable data-driven surrogates. *Expert Systems with Applications*, 202:117230.
- [31] Henckaerts, R., Côté, M.-P., Antonio, K., and Verbelen, R. (2021). Boosting insights in insurance tariff plans with tree-based machine learning methods. *North American Actuarial Journal*, 25(2):255–285.
- [32] Hickey, J., Metcalfe, P., Ridgeway, G., Schroedl, S., Southworth, H., and Therneau, T. (2016). *gbm3: Generalized Boosted Regression Models*. R package version 2.2.
- [33] Hofner, B., Mayr, A., and Schmid, M. (2016). gamboostlss: An r package for model building and variable selection in the gamlss framework. *Journal of Statistical Software*, 74(1):1–31.
- [34] Jordan, A., Krüger, F., and Lerch, S. (2017). Evaluating probabilistic forecasts with scoringRules. *arXiv preprint arXiv:1709.04743*.
- [35] Ke, G., Meng, Q., Finley, T., Wang, T., Chen, W., Ma, W., Ye, Q., and Liu, T.-Y. (2017). LightGBM: A highly efficient gradient boosting decision tree. *Advances in neural information processing systems*, 30:3147–3155.
- [36] Klein, N., Denuit, M., Lang, S., and Kneib, T. (2014). Nonlife ratemaking and risk management with bayesian generalized additive models for location, scale, and shape. *Insurance: Mathematics and Economics*, 55:225–249.
- [37] Lee, S. C. and Lin, S. (2018). Delta boosting machine with application to general insurance. *North American Actuarial Journal*, 22(3):405–425.

- [38] Lou, Y., Caruana, R., and Gehrke, J. (2012). Intelligible models for classification and regression. *Proceedings of the 18th ACM SIGKDD international conference on Knowledge discovery and data mining*, pages 150–158.
- [39] Lou, Y., Caruana, R., Gehrke, J., and Hooker, G. (2013). Accurate intelligible models with pairwise interactions. *Proceedings of the 19th ACM SIGKDD international conference on Knowledge discovery and data mining*, pages 623–631.
- [40] Luenberger, D. G. and Ye, Y. (2021). *Linear and nonlinear programming*. International series in operations research & management science. Springer, Cham, fifth edition edition.
- [41] März, A. (2019). XgboostLSS—an extension of XGBoost to probabilistic forecasting. *arXiv preprint arXiv:1907.03178*.
- [42] März, A. (2020). CatBoostLSS—an extension of CatBoost to probabilistic forecasting. *arXiv preprint arXiv:2001.02121*.
- [43] März, A. (2023). LightGBMLSS: An Extension of LightGBM to probabilistic modelling. <https://github.com/StatMixedML/LightGBMLSS>. GitHub repository, Version 0.4.0.
- [44] McFadden, D. (1974). Conditional logit analysis of qualitative choice behavior. *Frontier in Econometrics*, 10:105–142.
- [45] Meng, S., Gao, Y., and Huang, Y. (2022). Actuarial intelligence in auto insurance: Claim frequency modeling with driving behavior features and improved boosted trees. *Insurance: Mathematics and Economics*, 106:115–127.
- [46] Nori, H., Jenkins, S., Koch, P., and Caruana, R. (2019). Interpretml: A unified framework for machine learning interpretability. *arXiv preprint arXiv:1909.09223*.
- [47] Ohlsson, E. and Johansson, B. (2010). *Non-life insurance pricing with generalized linear models*, volume 174. Springer, New York.
- [48] Power, J., Côté, M.-P., and Duchesne, T. (2024). A flexible hierarchical insurance claims model with gradient boosting and copulas. *North American Actuarial Journal*, pages 772–800.
- [49] Priest, C. (2021). Predict workers compensation claims using highly realistic synthetic data. Accessed 16 November 2023.
- [50] Prokhorenkova, L., Gusev, G., Vorobev, A., Dorogush, A. V., and Gulin, A. (2018). CatBoost: unbiased boosting with categorical features. *Advances in neural information processing systems*, 31:6639–6649.
- [51] Rashmi, K. V. and Gilad-Bachrach, R. (2015). Dart: Dropouts meet multiple additive regression trees. *Journal of Machine Learning Research*, 38:489–497.
- [52] Rigby, R. A. and Stasinopoulos, D. M. (2005). Generalized additive models for location, scale and shape. *Journal of the Royal Statistical Society Series C: Applied Statistics*, 54(3):507–554.
- [53] Schapire, R. E. (1990). The strength of weak learnability. *Machine learning*, 5:197–227.
- [54] Shi, Y., Ke, G., Soukhavong, D., Lamb, J., Meng, Q., Finley, T., Wang, T., Chen, W., Ma, W., Ye, Q., Liu, T.-Y., and Titov, N. (2023). *LightGBM: Light Gradient Boosting Machine*. R package version 3.3.5.
- [55] Sigrist, F. (2021). Gradient and Newton boosting for classification and regression. *Expert Systems With Applications*, 167:114080.
- [56] So, B. (2024). Enhanced gradient boosting for zero-inflated insurance claims and comparative analysis of catboost, xgboost, and lightgbm. *Scandinavian Actuarial Journal*, 10:1013–1035.
- [57] So, B. and Valdez, E. A. (2024). Zero-inflated Tweedie boosted trees with CatBoost for insurance loss analytics. Available at SSRN 4876585.

- [58] Sprangers, O., Schelter, S., and de Rijke, M. (2021). Probabilistic gradient boosting machines for large-scale probabilistic regression. *Proceedings of the 27th ACM SIGKDD conference on knowledge discovery & data mining*, pages 1510–1520.
- [59] Srivastava, N., Hinton, G., Krizhevsky, A., Sutskever, I., and Salakhutdinov, R. (2014). Dropout: a simple way to prevent neural networks from overfitting. *The journal of machine learning research*, 15(1):1929–1958.
- [60] Turcotte, R. and Boucher, J.-P. (2024). GAMLSS for longitudinal multivariate claim count models. *North American Actuarial Journal*, 28(2):337–360.
- [61] Velthoen, J., Dombry, C., Cai, J.-J., and Engelke, S. (2023). Gradient boosting for extreme quantile regression. *Extremes*, 26(4):639–667.
- [62] Venables, W. N. and Ripley, B. D. (2002). *Modern Applied Statistics with S*. Springer, New York, fourth edition.
- [63] Wood, S. N. (2003). Thin plate regression splines. *Journal of the Royal Statistical Society Series B: Statistical Methodology*, 65(1):95–114.
- [64] Wüthrich, M. V. (2020). Bias regularization in neural network models for general insurance pricing. *European Actuarial Journal*, 10(1):179–202.
- [65] Wüthrich, M. V. and Buser, C. (2023). Data analytics for non-life insurance pricing. *Swiss Finance Institute Research Paper*, 16-68.
- [66] Xin, X. and Huang, F. (2024). Antidiscrimination insurance pricing: Regulations, fairness criteria, and models. *North American Actuarial Journal*, 28(2):285–319.
- [67] Xin, X., Huang, F., and Hooker, G. (2024). Why you should not trust interpretations in machine learning: adversarial attacks on partial dependence plots. *arXiv preprint arXiv:2404.18702*.
- [68] Yang, L. (2024). Double probability integral transform residuals for regression models with discrete outcomes. *Journal of Computational and Graphical Statistics*, 33:787–803.

## A Tuning strategy

We follow Algorithm 7 to tune hyperparameters with the five datasets used in claim frequency and severity modelling. We emphasize that all performance metrics are computed on a test set  $\mathcal{D}_{\text{test}}$  which is never seen in the tuning and the training process. To be specific, for dataset  $k$ , metric  $\psi$  and resulting model output from Algorithm 7, we compute

$$\frac{1}{|\mathcal{D}_{\text{test},k}|} \sum_{i \in \mathcal{D}_{\text{test},k}} \psi\{y_i, f_{k,\theta_k^*}(\mathbf{x}_i)\}.$$

Data partition is identical for all the algorithms.

Grid search is used for the maximum number of boosting iterations  $M$  and the tree depth  $d$ . We search over the same grid for these two hyperparameters across algorithms, but this grid is augmented by specific hyperparameters when necessary. We set the (constant) learning rate at 0.01, the sampling proportion at  $\delta = 0.75$ , and the minimum number of samples per leaf at 1% of the number of training observations.



---

**Algorithm 7:** Grid search scheme for tuning

---

**Input** : Datasets  $\mathcal{D}_1, \mathcal{D}_2, \mathcal{D}_3, \mathcal{D}_4$ , and  $\mathcal{D}_5$ , tuning grid `grid`, algorithm `algo`, and loss function  $\mathcal{L}$ .

- 1 **for**  $k = 1$  **to** 5 **do**
- 2     Sample  $\mathcal{D}_{\text{train},k}$ , a random subset of 85% of observations in  $\mathcal{D}_k$ .
- 3     Assign to  $\mathcal{D}_{\text{test},k}$  the remaining 15% of observations in  $\mathcal{D}_k$ .
- 4     Sample  $\mathcal{D}_{\text{hyp\_train},k}$ , a random subset of 80% of observations in  $\mathcal{D}_{\text{train},k}$ .
- 5     Assign to  $\mathcal{D}_{\text{val},k}$  the remaining 20% of observations in  $\mathcal{D}_{\text{train},k}$ .
- 6     **for** parameter combination  $\theta$  in `grid` **do**
- 7         Train model  $f_{k,\theta}$  using `algo` with  $\theta$  on  $\mathcal{D}_{\text{hyp\_train},k}$ .
- 8         Compute  $\text{score}_{k,\theta} = \frac{1}{|\mathcal{D}_{\text{val},k}|} \sum_{i \in \mathcal{D}_{\text{val},k}} \mathcal{L}\{y_i, f_{k,\theta}(\mathbf{x}_i)\}$ .
- 9     Choose the combination  $\theta_k^*$  which returns minimal  $\text{score}_{k,\theta}$ .
- 10    Train model  $f_{k,\theta^*}$  using `algo` with  $\theta_k^*$  on  $\mathcal{D}_{\text{train},k} = \mathcal{D}_{\text{hyp\_train},k} \cup \mathcal{D}_{\text{val},k}$ .
- 11 **Return** : For  $k \in \{1, \dots, 5\}$ , optimal hyperparameters  $\theta_k^*$ , trained model  $f_{k,\theta_k^*}$ .

---

## B Additional results

In Table 10, we show the training time in seconds for lognormal models. The average ranks are consistent with what we observe in Poisson models.

The adequacy of claim frequency models is assessed through DPIT residuals. These residuals should follow a uniform distribution if the model is adequate [68]. Tables 11–12 display the CRPS values for the Poisson and the NB2 models, respectively.

For severity models, the predicted distribution can be used directly to assess model adequacy with the CRPS. Tables 13–14 display the CRPS for the severity models.

The CI coverage on the test set for each model at levels 50%, 75%, 95% are presented in Tables 15–19. CI coverage is better for the lognormal models in the WorkComp dataset only, which is synthetic.

Table 10: Training time in seconds for lognormal models.

Model	Dataset					Avg. rank
	WorkComp	freMTPL	BelgianMTPL	pg15training	Emcien	
LightGBM	7	2	3	2	2	1.0
XGBoost	21	5	15	18	4	2.2
EGBM	26	6	24	78	6	3.8
GBM	78	40	19	25	5	4.0
CatBoost	43	16	28	83	29	4.0
PGBM	22	5	16	20	7	1.2
XGBoostLSS	46	16	36	41	9	2.2
NGBoost	495	38	46	121	66	2.6
cyc-GBM	743	240	266	1 188	105	4.6
XGBoostLSSd	556	278	251	1 082	399	4.4

Table 11: Uniform CRPS ( $\times 10^2$ ) of the DPIT residuals in Poisson models on the test set.

Model	Dataset				
	freMTPL	freMPL	BelgianMTPL	swauto	pg15training
LightGBM	16.299	16.33	16.487	16.666	16.64
XGBoost	16.302	16.03	16.286	16.671	16.43
EGBM	16.354	16.62	16.494	16.683	16.73
GBM	16.332	16.22	16.502	16.685	16.80
CatBoost	16.294	16.32	16.496	16.665	16.62
XGBoostLSS	16.298	<b>15.96</b>	<b>16.283</b>	16.672	<b>16.38</b>
NGBoost	<b>16.098</b>	15.97	16.461	16.691	16.70
cyc-GBM	16.628	16.30	16.610	16.665	16.65
XGBoostLSSd	16.323	16.60	16.452	<b>16.649</b>	16.40

Table 12: Uniform CRPS ( $\times 10^2$ ) of the DPIT residuals in NB2 models on the test set.

Model	Dataset				
	freMTPL	freMPL	BelgianMTPL	swauto	pg15training
LightGBM	16.316	15.86	16.491	16.6780	<b>16.577</b>
XGBoost	<b>16.320</b>	16.01	<b>16.488</b>	<b>16.5753</b>	16.599
EGBM	16.360	16.19	16.496	16.6910	16.681
GBM	16.345	<b>15.81</b>	16.505	16.6856	16.732
CatBoost	16.321	15.91	16.500	16.6729	16.580
XGBoostLSS	16.734	17.38	16.668	16.6989	16.636
NGBoost	16.710	17.30	16.672	16.6988	16.682
cyc-GBM	16.898	17.05	16.779	16.7396	16.669
XGBoostLSSd	16.745	17.36	16.609	16.7214	16.646

Table 13: CRPS in lognormal models on the test set.

Model	Dataset				
	WorkComp	freMTPL	BelgianMTPL	pg15training	Emcien
LightGBM	0.586	0.768	1.157	0.810	0.216
XGBoost	0.592	0.779	1.133	0.816	0.263
EGBM	0.588	0.791	1.140	0.818	0.264
GBM	0.619	0.785	1.142	0.868	0.262
CatBoost	0.652	0.790	1.140	0.808	0.210
PGBM	0.746	0.803	1.146	0.865	0.238
XGBoostLSS	<b>0.573</b>	0.659	0.816	<b>0.672</b>	<b>0.187</b>
NGBoost	0.580	<b>0.658</b>	<b>0.805</b>	0.673	0.189
cyc-GBM	0.578	0.663	0.860	0.675	0.188
XGBoostLSSd	0.574	0.659	0.806	0.679	0.190

Table 14: CRPS in gamma models on the test set.

Model	Dataset				
	WorkComp	freMTPL	BelgianMTPL	pg15training	Emcien
LightGBM	6 926	1 204.8	545.6	<b>336.10</b>	64.4
XGBoost	6 955	1 203.9	545.7	336.18	64.5
EGBM	6 953	1 203.3	546.2	336.94	63.9
GBM	7 094	1 207.4	546.4	342.23	64.6
CatBoost	6 920	1 201.1	545.5	336.26	63.1
XGBoostLSS	6 939	1 204.5	545.4	336.97	66.1
NGBoost	<b>6 925</b>	<b>1 203.3</b>	<b>544.0</b>	336.93	58.0
cyc-GBM	6 935	1 198.9	544.7	338.80	<b>57.3</b>
XGBoostLSSd	7 064	1 206.7	547.3	339.91	63.1

Table 15: Coverage (in %) of CI at levels 50%, 75%, and 95% on the test BelgianMTPL set.

Model	Lognormal distribution			Gamma distribution		
	50%	75%	95%	50%	75%	95%
LightGBM	3.97	6.59	14.27	30.22	71.42	94.86
XGBoost	2.21	4.04	6.82	29.33	75.36	96.25
EGBM	2.28	4.12	7.12	29.63	75.28	96.37
GBM	1.87	3.63	6.40	27.38	74.79	96.48
CatBoost	2.13	3.97	6.67	29.74	75.24	96.22
XGBoostLSS	27.90	65.62	95.33	29.51	77.49	96.67
NGBoost	28.73	73.33	97.83	29.85	78.61	96.59
cyc-GBM	17.68	41.39	82.55	30.00	77.64	96.52
XGBoostLSSd	29.51	71.95	97.45	31.42	75.62	95.96

Table 16: Coverage (in %) of CI at levels 50%, 75%, and 95% on the test WorkComp set.

Model	Lognormal distribution			Gamma distribution		
	50%	75%	95%	50%	75%	95%
LightGBM	57.90	80.36	94.68	56.75	81.92	93.80
XGBoost	55.57	78.02	93.84	60.96	87.32	95.19
EGBM	55.96	78.83	94.21	61.85	87.31	95.17
GBM	50.85	74.23	92.72	54.01	85.61	95.38
CatBoost	40.38	60.40	84.56	60.25	86.25	94.78
XGBoostLSS	47.08	70.91	89.82	61.74	87.21	94.71
NGBoost	52.50	77.21	93.84	59.91	87.77	94.82
cyc-GBM	45.16	69.02	88.62	58.91	88.41	95.12
XGBoostLSSd	48.35	69.96	90.85	60.28	86.42	95.23

Table 17: Coverage (in %) of CI at levels 50%, 75%, and 95% on the test freMTPL set.

Model	Lognormal distribution			Gamma distribution		
	50%	75%	95%	50%	75%	95%
LightGBM	16.84	27.27	44.20	62.93	77.71	94.48
XGBoost	11.89	21.66	37.32	65.54	79.58	95.01
EGBM	7.53	15.01	29.10	65.75	79.95	95.10
GBM	10.02	19.56	34.30	66.33	79.95	95.40
CatBoost	7.55	16.21	30.76	66.35	79.88	95.29
XGBoostLSS	63.05	77.55	92.24	66.24	80.28	95.40
NGBoost	61.48	76.56	91.48	65.01	79.10	94.73
cyc-GBM	58.38	73.05	88.73	59.35	74.36	90.02
XGBoostLSSd	62.03	77.14	91.69	65.31	79.58	94.90

Table 18: Coverage (in %) of CI at levels 50%, 75%, and 95% on the test pg15training set.

Model	Lognormal distribution			Gamma distribution		
	50%	75%	95%	50%	75%	95%
LightGBM	12.40	20.62	35.47	49.78	74.43	93.74
XGBoost	11.31	19.59	33.46	50.05	74.37	93.42
EGBM	11.05	19.37	34.28	49.84	74.10	93.63
GBM	7.02	10.55	20.00	50.82	75.19	93.91
CatBoost	12.57	20.84	35.15	49.84	74.92	93.63
XGBoostLSS	51.58	78.56	94.56	51.03	75.84	94.06
NGBoost	51.25	78.02	94.34	49.78	73.50	93.47
cyc-GBM	49.78	74.70	93.15	47.61	71.82	92.22
XGBoostLSSd	47.44	72.47	91.57	45.97	70.24	91.57

Table 19: Coverage (in %) of CI at levels 50%, 75%, and 95% on the test Emcien set.

Model	Lognormal distribution			Gamma distribution		
	50%	75%	95%	50%	75%	95%
LightGBM	89.13	95.33	98.67	68.87	84.07	92.93
XGBoost	88.53	95.27	98.73	71.00	85.73	94.20
EGBM	88.27	95.40	98.67	69.67	84.87	93.47
GBM	88.27	95.53	98.60	71.00	85.47	94.67
CatBoost	99.80	100.00	100.00	69.80	84.93	93.33
XGBoostLSS	47.53	75.47	93.93	79.73	92.00	98.73
NGBoost	44.20	71.20	93.00	50.80	75.53	95.00
cyc-GBM	38.00	58.13	78.67	36.33	57.67	78.20
XGBoostLSSd	43.73	73.40	93.87	73.67	89.60	98.40